

# Lightning declines over shipping lanes following regulation of fuel sulfur emissions

Chris J Wright<sup>a</sup>, Joel A Thornton<sup>a</sup>, Lyatt Jaeglé<sup>a</sup>, Yang Cao<sup>b</sup>, Yannian Zhu<sup>b</sup>, Jihu Liu<sup>b</sup>, Randall Jones II<sup>a</sup>, Robert H Holzworth<sup>c</sup>, Daniel Rosenfeld<sup>d</sup>, Robert Wood<sup>a</sup>, Peter Blossey<sup>a</sup>, and Daehyun Kim<sup>a</sup>

<sup>a</sup>University of Washington, Department of Atmospheric Sciences, Seattle, WA, 98195

<sup>b</sup>Nanjing University, School of Atmospheric Sciences, Nanjing, China, 210023

<sup>c</sup>University of Washington, Department of Earth and Space Sciences, Seattle, WA, 98195

<sup>d</sup>The Hebrew University of Jerusalem, Institute of Earth Sciences, Jerusalem, Israel, 91904

<sup>e</sup>Seoul National University, Department of Atmospheric Science, Seoul, South Korea, 08820

## Abstract

Aerosol interactions with clouds represent a significant uncertainty in our understanding of the Earth system. Deep convective clouds may respond to aerosol perturbations in several ways that have proven difficult to elucidate with observations. Here, we leverage the two busiest maritime shipping lanes in the world, which emit aerosol particles and their precursors into an otherwise relatively clean tropical marine boundary layer, to make headway on the influence of aerosol on deep convective clouds. The recent seven-fold change in allowable fuel sulfur by the International Maritime Organization allows us to test the sensitivity of the lightning to changes in ship plume aerosol size distributions. We find that, across a range of atmospheric thermodynamic conditions, the previously documented enhancement of lightning over the shipping lanes has fallen by over 40%. The enhancement is therefore at least partially aerosol-mediated, a conclusion that is supported by observations of droplet number at cloud base, which show a similar decline over the shipping lane. These results have fundamental implications for our understanding of aerosol-cloud interactions, suggesting that deep convective clouds are impacted by the aerosol number distribution in the remote marine environment.

**Significance:** Aerosol particles, also known as particulate matter, are a key ingredient in cloud formation. Because clouds exert a large forcing on solar radiation and fresh water, the mechanisms of aerosol-cloud interactions are of significant interest. However, the complexity of the interaction between aerosol and clouds has made it difficult to study, particularly in deep convective clouds, or thunderstorms. To better understand the mechanisms by which aerosol influences thunderstorms, we look at the two busiest shipping lanes in the world, where recent regulations have reduced sulfur emissions by nearly an order of magnitude. We find that the reduction in emissions has been accompanied by a dramatic decrease in both lightning and the number of droplets in clouds over the shipping lanes.

By acting as cloud condensation nuclei (CCN), aerosol particles influence clouds and, in turn, the Earth's energy balance. These aerosol interactions with clouds represent a significant uncertainty in our understanding of the Earth's climate (1). Shipping lanes can be used as a natural experiment to reduce that uncertainty. Fuel combustion by maritime shipping vessels in the open ocean leads to the emission of aerosol particles and associated precursors, such as SO<sub>2</sub>, into

relatively clean marine air. These emissions can perturb low-level marine stratus cloud droplet number distributions and related macrophysical properties, such as cloud albedo and lifetime, by increasing CCN concentrations (2–5).

Deep convective cloud (DCC) systems, commonly known as cumulonimbus or thunderstorms when lightning is generated, occur throughout the tropics, and are essential to the Earth's water and energy cycles. In the tropics and some mid-latitude regions, the majority of precipitation and extreme weather is associated with DCCs (6). However, there is no strong consensus on the mechanisms or magnitudes of aerosol particle impacts on DCCs (7–9). Thornton et al (10) documented a potential case of persistent maritime aerosol-DCC interactions analogous to the stratocumulus ship tracks, with the discovery of enhancements in lightning located over the two busiest shipping lanes in the world, which pass through the Indian Ocean and South China Sea (Fig. 1). Lightning results from cloud electrification, which in turn requires sufficient updraft velocity, vertical ice fluxes, and super-cooled liquid water in the mixed-phase region of a DCC to induce and sustain charge separation (11, 12). Several relevant mechanisms have been proposed by which aerosol particle could enhance lightning frequency over the polluted shipping corridors, all of which involve additional aerosol particles from ship emissions causing enhanced cloud droplet nucleation (13), which subsequently leads to either 1) a perturbation to the super-cooled liquid water and ice hydrometeor distributions in the mixed-phase region of DCC (14–16); or 2) an increase in the frequency or intensity of deep convection due to changes in the vertical distribution of humidity (17) or heating (18, 19). Some combination of 1 or 2 is also possible.

In January 2020, the International Maritime Organization (IMO) reduced the amount of allowable sulfur in fuel by a factor of seven, from 3.5% to 0.5% to curb effects of the maritime shipping industry on air pollution (20). After similar regulations of fuel sulfur content, a study of ship plumes in the Baltic Sea documented a shift in the aerosol size distribution to smaller sizes (21). Recent analyses of shallow stratocumulus marine clouds over shipping lanes find changes to cloud brightness, droplet number, and droplet size, amounting to a globally averaged radiative forcing perturbation of O(0.1 Wm<sup>-2</sup>) associated with the IMO regulation, presumably due to the shift in aerosol size distribution (3, 22, 23). To date, no study has quantified the impact of the IMO regulation on DCCs.

Given that shallow clouds have exhibited a shift in droplet size distribution since the IMO regulation of sulfur, so too might DCCs, with downstream effects on mixed-phase

microphysics, dynamics, and lightning. Here, we investigate how recent changes in ships’ fuel sulfur content impact lightning over the shipping lanes in the tropical Indian Ocean and South China Sea. We show that the shipping lane lightning enhancement decreases significantly with the onset of the IMO regulation and that this decrease in lightning is persistent in time across a range of atmospheric conditions. We further show that the mean cloud droplet number concentration of shallow warm clouds over the Indian Ocean shipping lane was enhanced before the IMO regulation and also exhibits a decrease since the IMO regulation. Finally, we discuss the implications of these results for the mechanisms of shipping lane lightning enhancement and for aerosol particle-DCC interactions generally.

## Results

Lightning stroke density, measured by the World Wide Lightning Detection Network (WWLLN) over both the Indian Ocean and South China Sea shipping lanes (hereafter “the shipping lanes”), has decreased since the onset of the 2020 IMO regulation of sulfur emissions (Figure 1). Relatively constant ship traffic (Figure S1) (24), paired with continuous observations of lightning from WWLLN, provide large samples to generate robust statistics. The Port of Singapore accounts for roughly 20% of the world’s bunkering fuel demand, and the two primary shipping lanes it services have nearly an order of magnitude higher traffic than other shipping lanes in the region (and around the world) (top panel) (25). We show that there is an enhancement in mean lightning stroke density associated with these shipping lanes, consistent with previous work of Thornton et al, but updated for the time period of 2010 to 2019 in Figure 1 (middle panel). Since 2020, lightning over the shipping lanes has declined by about 1 stroke  $\text{km}^{-2} \text{ year}^{-1}$  as indicated by the difference in lightning stroke density between the mean of years 2020-2023 and that of 2010-2019 shown in Figure 1 (bottom panel). While some of the largest absolute declines in lightning since 2020 occur over the shipping lanes, lightning has increased or decreased in other parts of this region, suggesting that changes in the dynamic and thermodynamic context for convection over these shipping lanes should be taken into account.

We first examine changes in the lightning stroke density enhancement over the shipping lanes using two basic controls on the background meteorology: 1) we only consider samples of precipitating clouds, using IR and radar-calibrated microwave precipitation measurements from integrated multi-satellite retrievals (IMERG) (27–29); and 2) we restrict analyses to seasons for which the conditions for lighting are favorable in each region (November to April in the Indian Ocean; June to November in the South China Sea). Given these controls, we then composite the observations as a function of distance to the shipping lanes, the center of which we define as the peak in shipping emissions from the EDGAR emissions inventory (see Methods). Mean lightning as a function of distance from the shipping lanes before (pre-IMO) and after (post-IMO) the 2020 regulation shows that the clear enhancement, between approximately 150km south to 150km north of the shipping lanes, has decreased since the regulation (Figure 2a). As before, lightning has also fallen region-wide, particularly to

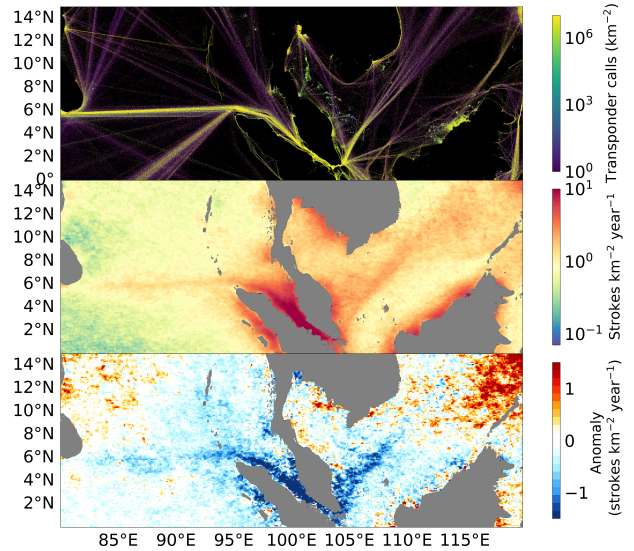


**Fig. 1.** (top) Map showing the total number of Automatic Identification Systems (AIS) transponder calls from 2015-2021, used by maritime vessels for collision avoidance. Data from the IMF World Seaborne Trade dataset (26). (middle) Climatological mean lightning stroke density near the Port of Singapore (2010-2019). (bottom) Difference of the post-regulation period (2020-2023) lightning stroke density from the 2010-2019 climatology above

the south of the shipping lanes, suggesting changes to the background (non-aerosol) drivers of lightning.

To account for natural variability in the frequency and intensity of convection in the region, we construct an estimate of the natural (unperturbed) annual lightning by regressing the observed annual lightning at a given distance from the shipping lane against three variables known to relate to lightning stroke density: Convective Available Potential Energy (CAPE, discussed further below) and precipitation rates (30), as well as the annual mean Oceanic Niño Index (ONI). All variables are subjected to the same two controls listed above — precipitating (except ONI) and restricted to the high lightning season. The influence of El Niño is assumed to be uniform across the domain for a given year. The regressed variables explain roughly 33% of variance of the annual means. The regressed predictions for lightning are then removed from the observed annual mean, leaving the anomalous mean lightning stroke density, the time series of which is shown as a function of distance from the shipping lane in Figure 2b. Also shown in the right panel of Figure 2b is the monthly fraction of fuel sales at the Port of Singapore that are high- and low-sulfur.

Prior to the IMO regulation, essentially 100% of fuel sold at the port was the high sulfur type; correspondingly, the lightning anomaly over the shipping lane was 4.0 strokes  $\text{km}^{-2} \text{ year}^{-1}$  on average and never fell below 3 strokes  $\text{km}^{-2} \text{ year}^{-1}$  for more than one year at a time. Then, as evidenced by the bunkering fuel sales, adoption of the new regulation was immediate in 2020, such that high sulfur fuel has comprised less than 35% of fuel sold at the Port of Singapore. Since the adoption of lower-sulfur fuels in January 2020, the shipping lane lightning enhancements have declined significantly: the

anomaly has fallen to 1.8 strokes  $\text{km}^{-2} \text{ year}^{-1}$  on average, with none of the 4 years reaching higher than 2.2 strokes  $\text{km}^{-2} \text{ year}^{-1}$ . That is, the enhancement has declined by approximately 50%.

The preceding analysis relies on an assumption that the annual mean CAPE, precipitation, and ONI account for year-to-year variations in the regional drivers of convection and lightning. To further control for higher-frequency variations in the large-scale thermodynamic conditions, we examine the lightning enhancement in a 2-dimensional CAPE and precipitation space, populated by 3-hourly coincident observations of CAPE, precipitation, and lightning. Romps et al. (30) showed that  $\text{CAPE} \times \text{precipitation}$  is a reasonable proxy for lightning frequency over land, and Cheng et al (31) showed that, after adjusting for a CAPE threshold,  $\text{CAPE} \times \text{precipitation}$  is a reasonable proxy for tropical oceanic lightning frequency. CAPE provides an estimate of the energetic potential for deep convection and the associated updraft strength while precipitation rate indicates both the presence of a storm and a measure of its intensity. By partitioning 3-hourly lightning observations into CAPE and precipitation bins, we control for regional and temporal variations in the environmental conditions which influence lightning to further isolate the impact of the shipping lane on stroke density.

We compute lightning frequency in each CAPE-Precip bin using data from a region centered over each shipping lane and from reference regions adjacent to the shipping lanes, similar to those in (10) (Figure S2). We then compute a relative enhancement in lightning over the shipping lanes before and after the IMO regulation onset by taking the difference between corresponding CAPE-Precip bin-means in the shipping lane and reference box histograms. The shipping lane lightning enhancements in the CAPE-Precip space are shown in Figure 3. Before the IMO regulation (Pre-IMO), a strong shipping lane lightning enhancement existed in nearly every thermodynamic setting (e.g., in each CAPE-Precip bin, Figure 3a,d) for both shipping lanes.

Since the IMO regulation (Post-IMO), both shipping lanes exhibit significantly weaker lightning enhancements across most CAPE-Precip regimes (Figure 3b,e). The bin-by-bin differences between the Pre and Post-IMO lightning enhancement histograms for each shipping lane are shown in Figure 3 (c and f). For the vast majority of CAPE-Precip bins with statistically significant differences, the lightning enhancement Post-IMO has been weaker than that Pre-IMO. On average across all CAPE-Precip conditions, the lightning enhancement has decreased by 76% and by 47% for the Indian Ocean and South China Sea shipping lanes, respectively. (Figure 3c,f).

Total fuel sales at the Port of Singapore, which we take as a proxy for ship traffic and combustion in the shipping lanes, have been either stable or increasing since the 2020 regulation. The decline in the lightning enhancement since 2020 is therefore most consistent with the change in emissions composition in 2020 associated with the IMO regulation. If decreasing sulfur emissions over the shipping lanes have reduced the number of viable CCN and disrupted the mechanism for lightning enhancement, there should be a corresponding change in warm cloud microphysics. To test for such a change, we use Moderate Resolution Imaging Spectroradiometer (MODIS) satellite observations of cloud

droplet number ( $N_d$ ) in warm (shallow) clouds over the Indian Ocean shipping lane (where the influence of land is weaker and ship emissions are stronger) during the high-lightning season. The retrievals of  $N_d$  follow the method outlined in Zhu et al (32), such that we sample only the brightest, most active warm clouds to ensure that assumptions of adiabatic ascent are as realistic as possible. Due to the optical thickness of DCC, these retrievals can only be done for shallow warm clouds, and therefore this analysis samples a different set of conditions than the lightning observations. We thus assume that the behavior of  $N_d$  in shallow cumulus clouds from the same region is related to, though not necessarily a direct proxy for,  $N_d$  at cloud base in DCC. Unlike WWLLN lightning observations, which are influenced by the frequency of deep convection and therefore generally trend toward the ITCZ, the  $N_d$  retrievals mostly represent perturbations to CCN below shallow cumulus, consistently trending toward land.

In Figure 4, we show that prior to the IMO regulation,  $N_d$  generally increases toward land (north), with a clear enhancement in  $N_d$  over the shipping lane. This  $N_d$  perturbation is roughly 5-10% above the background (here taken simply as the average of droplet concentrations 150km north and 150km south), which is similar in magnitude to the shipping lane perturbation detected by Diamond (2) in stratocumulus clouds in the Southeast Atlantic. Since the IMO regulation,  $N_d$  has declined region-wide, and the enhancement in  $N_d$  over the shipping lane has become essentially undetectable. This corresponding decline in  $N_d$  over the shipping lane establishes additional support for the declining lightning enhancement being related to a shift in aerosol particle number-size distributions, and consequently CCN distributions over the shipping lanes induced by the IMO regulation.

## Implications

We find that a previously identified enhancement in lightning stroke density over the two major shipping routes near the Port of Singapore has declined by over 40% since 2020, when the IMO regulation aimed at reducing sulfur emissions from maritime shipping came into effect. Controlling for natural variations in environmental conditions, we observe that a decline in the lightning enhancement has taken place across a range of thermodynamic regimes. The statistically robust response of lightning coincident with the onset of the IMO regulation suggests that the mechanism for the enhancement is mostly aerosol-mediated. While the ships themselves do likely act as attractors of lightning due to their prominence over the flat ocean (33), there is not evidence of a significant change in the number of ships traversing these shipping lanes over this time period (Figure S1). Further, that there was an independently observed perturbation to  $N_d$  over the Indian Ocean shipping lane prior to the IMO regulation that has since nearly vanished is indicative of a coincident change in CCN over the region. The correlated behavior between  $N_d$  and lightning lends credence to the set of CCN-mediated hypotheses proposed for invigoration of lightning (14, 17, 18).

Precisely how elevated  $N_d$  might lead to enhanced lightning remains unresolved. Both the pre-IMO and post-IMO perturbations to  $N_d$  are smaller than the enhancements of lightning, which may suggest non-linear relationships between  $N_d$ , secondary ice processes, and charge separation,



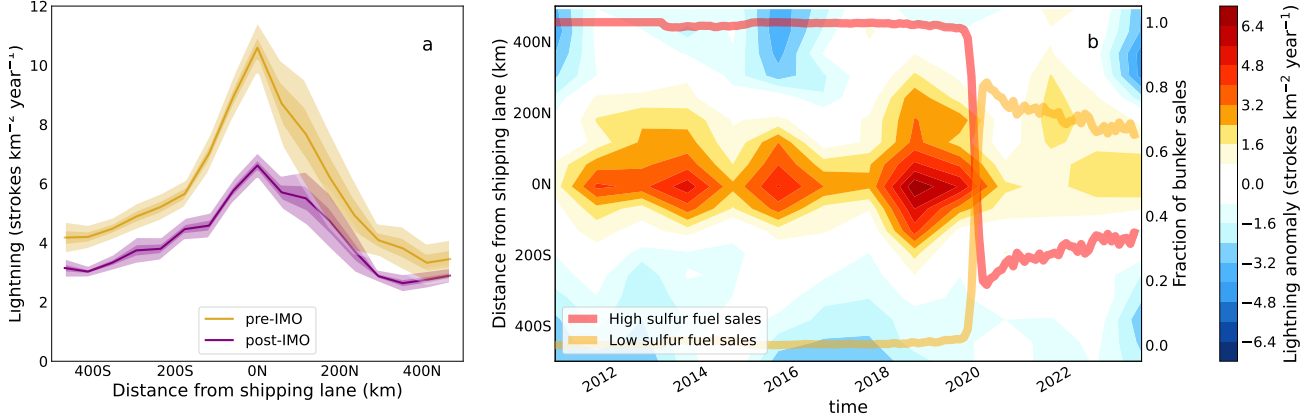


**Fig. 2.** (a) Lightning stroke density as a function of distance to the shipping lanes before and after the IMO regulation. Shading represents  $\pm 2SE$  and  $\pm 3SE$  (b) Hovmöller diagram of the annual mean lightning anomaly from the linear regression using Convective Available Potential Energy, precipitation, and Oceanic Niño Index from reanalysis data and observations (see text and SI for more details).

or additional interactions between DCC and aerosol acting as ice nucleating particles (INP) that covary with the CCN that enhance  $N_d$ . Moreover, we currently lack the *in situ* observations of aerosol size distributions needed to assess how the IMO regulations have led to changes in CCN in these regions for the conditions of DCC. Given the strong updrafts in DCC, aerosol particles can experience very high supersaturation with respect to liquid water, enabling ultrafine aerosol to act as CCN, and potentially enhancing lightning without an enhancement of  $N_d$  in the less vigorous, warm clouds detectable by our methods.

Seppala et al (21) find that, in the case of a factor of 10 reduction in sulfur in ship fuel, in-plume aerosol size distributions generally shift toward lower sizes and concentrations of ultrafine particles decrease very little, or even increase as a result of the IMO regulation. As such, if the observed shipping lane lightning enhancement were the result of ultrafine particles invigorating convection (18), we would expect little change in the lightning enhancement with the IMO regulation, which is inconsistent with the decrease in lightning stroke density that we observe. We therefore conclude that the lightning enhancement over the shipping lane prior to the IMO regulation is more likely caused mostly by fine mode aerosol perturbations to 1) cloud microphysics, such as elevated supercooled liquid water concentrations or rime splintering (14) or 2) invigoration of updrafts by heightened free tropospheric humidity in polluted clouds wrought by warm rain suppression (17). That said, enhanced ultrafine particle activation to cloud drops in DCC over the shipping lanes could be an explanation for the persistent, but lower, lightning enhancement over the shipping lanes post-IMO.

We use the regulation of ship fuel sulfur to identify and assess connections between maritime shipping emissions, aerosol particle size and composition, DCC microphysics, and lightning stroke density. Further work is needed to clarify these connections and to quantify the relative roles of dynamic and microphysical responses, but our findings suggest these regions remain a useful testbed for understanding aerosol impacts on deep convective cloud and lightning. Although satellite-

based radar observations of DCC microphysics are available, the spatial and temporal coverage is not yet sufficient to test whether there have been changes since the IMO. However, as time passes, statistical strength for the comparison between the two periods will increase, enabling a broader assessment of the DCC response to aerosol particles assuming maritime shipping emissions in the region remain in compliance with the IMO regulations.

## Materials and Methods

Lightning stroke density observations come from the Worldwide Lightning Location Network (WWLLN), a ground-based lightning detection network with continuous global coverage of lightning at a resolution of 10km (34). WWLLN uses very low frequency radio impulses (3-30 kHz) that, upon emission from a lightning stroke, propagates between the Earth-ionosphere waveguide and disperses into a wave train. The phase and frequency of that wave train determine the time of group arrival at three or more measurement stations, which can be used to back out the location of the stroke. While the detection efficiency for individual events is lower than satellite-based methods, continuous observations for more than a decade offer much more statistical power over our region of interest.

We use integrated multi-satellite retrievals for GPM (IMERG) precipitation rates (27) and European Centre for Medium-Range Weather Forecasts (ECMWF) ReAnalysis-5th Generation (ERA5) atmospheric reanalyses (35) CAPE to compare the enhancement across various thermodynamic conditions. IMERG precipitation combines microwave and radar retrievals from TRMM and the GPM constellation. In ERA5, a value for CAPE is calculated for every departing level between the surface and 350hPa as follows:

$$CAPE = \int_{z_{dep}}^{z_{top}} g \left( \frac{\theta_{ep} - \bar{\theta}_{esat}}{\bar{\theta}_{esat}} \right) dz$$

where  $z_{dep}$  is the departing level,  $z_{top}$  is the level of neutral buoyancy,  $\theta_{ep}$  is the virtual potential temperature of the parcel, and  $\bar{\theta}_{esat}$  is the saturation virtual potential temperature of the

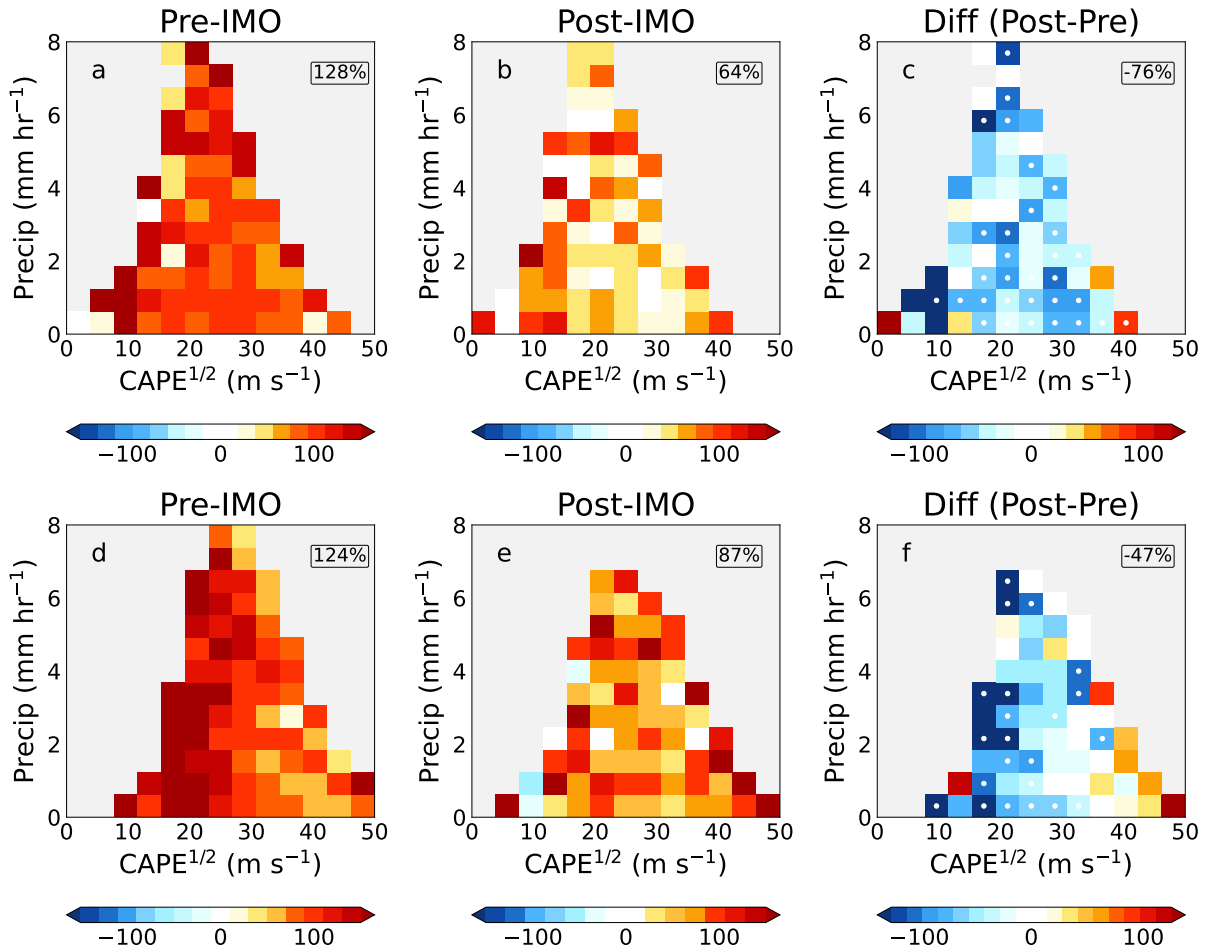


**Fig. 3.** Mean shipping lane percent enhancement in lightning stroke density (i.e., the relative difference in lightning over the shipping lane from that over immediately adjacent regions, see text), shown as colored pixels, binned by square root of CAPE reanalysis data (x-axis) and precipitation observations (y-axis) for the Indian Ocean (a)–(c) and South China Sea (d)–(f) shipping lanes. Enhancements since the regulation (b, e) are lower than before the regulation (a, d). The difference between post- and pre-IMO periods of the shipping lane lightning enhancements are represented in (c, f), where stippled bins indicate significance ( $p$  less than 0.05).

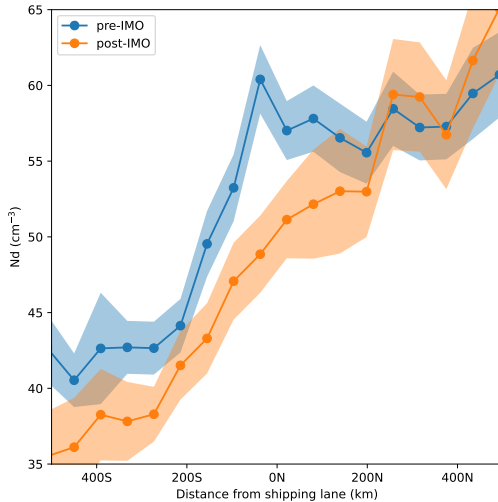


**Fig. 4.** Warm cloud-base droplet number ( $N_d$ ) concentrations over the Indian Ocean, derived from MODIS observations of optical depth and effective radius following the procedure from (32). The pre-IMO regulation period is 2010-2019. Note the general increasing trend northward through the domain toward greater land influence, and the broad localized enhancement over the shipping lane prior to the regulation. Shading represents  $\pm 2SE$ .

environment. Once CAPE has been calculated for all levels, the most unstable layer is selected. We use  $CAPE^{1/2}$ , which is directly proportional to  $w_{max}$ , the theoretical maximum vertical velocity achievable at a location given the stability of the atmosphere. This follows from the proportionality between kinetic energy and the square of velocity. Further discussion of CAPE as it relates to lightning can be found in (31) and (30).

Lightning in Figure 1 is shown on  $0.1^\circ \times 0.1^\circ$  grid, calculated from 3-hourly lightning stroke densities. For subsequent calculations of the enhancement (Figures 2-3) all data (CAPE, precipitation, and lightning) is 3-hourly and mapped to a  $0.5^\circ N \times 0.625^\circ E$  grid to minimize collocation errors and noise, and for comparison with MERRA-2 aerosol and meteorological reanalysis fields. Smoothly varying data (CAPE) is remapped bilinearly, while non-smoothly varying data (precipitation and lightning) are remapped conservatively (see (36) and sources therein for further detail on regridding practices). To provide some basic control for thermodynamic and meteorological variability, we only consider precipitating clouds (precipitation greater than 0.1mm/hr). We use data from 2010 onward, as WWLLN detection efficiency was still increasing rapidly prior to 2010. The shipping lanes are defined as regions where the Emissions Database for Global Atmospheric Research (EDGAR)  $PM_{2.5}$  shipping emissions are greater than  $5 \times 10^{-12} \text{ kg m}^{-2} \text{ s}^{-1}$  (37). To remove influence from katabatic flows and sea-breeze driven convergence, we only consider the larger blue regions outlined in Figure S2. This notably removes the straight of Malacca, a region with both very high shipping emissions and active convection. There, surface convergence from land-based precipitation outflows on Sumatra and Malaysia and the adjacent landmasses make it challenging

to establish a counterfactual, given the well-known land-ocean contrast in lightning stroke rates.

For Figure 2, the lightning stroke density ( $F$ ) as a function of time ( $t$ ) and distance from shipping lane ( $y$ ) from the entire record is regressed as:

$$F(y, t) = \beta * X(y, t) + \epsilon$$

where  $X$  is the vector of predictors, CAPE, precipitation, and ONI,  $\beta$  is the vector of coefficients.  $\epsilon$  is the residual or "anomaly" that is shown in the figure. This anomaly represents the difference between the lightning one would expect given the environmental conditions ( $\beta * X$ ) (see Figure S3) and the observed lightning ( $F$ ).

We utilized the "brightest 10%" method (32, 38) to obtain reliable  $N_d$  (cloud droplet number concentration) retrievals from MODIS Aqua across our target domain from 2010 to 2023. This method involves selecting the brightest 10% of clouds within each scene to calculate  $N_d$  values for every  $0.5^\circ \times 0.5^\circ$  grid box. The validity of this retrieval method has been corroborated through comparisons with ship-based observations (39, 40).  $N_d$  is computed using the cloud effective radius ( $r_e$ ) and cloud optical depth ( $\tau$ ), as described by the equation:

$$N_d = \frac{\sqrt{5}}{2\pi k} \left( \frac{f_{ad} C_w \tau}{Q_{ext} \rho_w r_e^5} \right)^{\frac{1}{2}}$$

where  $k$  represents the volume radius ratio of cloud droplets ( $r_v$ ) to  $r_e$  ( $k = (r_v/r_e)^3 = 0.8$ ). The term  $f_{ad}$  denotes the adiabatic fraction, for which we assumed a constant value of 1 in our study, due to the absence of more refined alternatives (41, 42).  $C_w$  signifies the adiabatic cloud water condensation rate within an ascending cloud parcel, expressed in grams per cubic meter per meter ( $\text{g m}^{-3} \text{ m}^{-1}$ ). The extinction efficiency factor,  $Q_{ext}$ , is assumed to be 2, and  $\rho_w$  is the density of water. To enhance the accuracy of our  $N_d$  estimations for each  $0.5^\circ \times 0.5^\circ$  grid box, we excluded pixels where the solar zenith angle exceeded 65 degrees (Grosvenor and Wood, 2014). We also excluded of scenes containing mixed-phase, ice, or multilayer clouds. Consequently, after applying these filtering criteria, the remaining dataset comprised less than 1% of multilayer cloud pixels in any given grid. We use only the Indian Ocean shipping lane to maximize signal-to-noise, as the South China Sea has a much weaker signal due to its proximity to land and lower ship emissions. Inclusion of the South China Sea in the analysis does not alter the results.

## Data, Materials, and Software

ERA5 CAPE may be downloaded using the Copernicus API at [cds.climate.copernicus.eu](https://cds.climate.copernicus.eu). IMERG Precipitation is available for download at [disc.gsfc.nasa.gov](https://disc.gsfc.nasa.gov). WWLLN data is available at [WWLLN.net](https://wwlln.net). ONI index is available at [psl.noaa.gov/data/correlation/oni.data](https://psl.noaa.gov/data/correlation/oni.data). MODIS Aqua (MYD06) retrievals are available at [ladsweb.modaps.eosdis.nasa.gov](https://ladsweb.modaps.eosdis.nasa.gov). Global ship traffic density is available at: [datacatalog.worldbank.org/search/dataset/0037580/Global-Shipping-Traffic-Density](https://datacatalog.worldbank.org/search/dataset/0037580/Global-Shipping-Traffic-Density). Analysis and plotting available at [10.5281/zenodo.11373991](https://doi.org/10.5281/zenodo.11373991) (43)

## Author Contributions

Analysis: CJW. Writing: CJW and JAT. Conceptualization and methodological development: CJW, JAT, LJ, and RW. Nd retrievals by: YC, YZ, JL. Additional expertise provided by RH, DR, RJ, PN, and DK

## Acknowledgements

This work was funded by a grant from the U.S. National Science Foundation (AGS-2113494). Additional funding included (in order of authorship): Natural Science Foundation of China grant 42075093 (YC, YZ, JL), BSF Grant 2020809 (DR), NASA/UMBC grant NASA0144-01 (RW), NSF grant AGS-1912130 (PN), and New Faculty Startup Fund from Seoul National University (DK). The authors wish to thank the World Wide Lightning Location Network (<http://wwlln.net>), a collaboration among over 50 universities and institutions, for providing the lightning location data used in this paper.

## Bibliography

- Olivier Boucher, D. Randall, Paulo Artaxo, C. Bretherton, Graham Feingold, Piers Forster, Veli-Matti Kerminen, Y. Kondo, H. Liao, Ulrike Lohmann, P. Rasch, S. Satheesh, S. Sherwood, B. Stevens, and X. Zhang. Clouds and Aerosols. pages 571–892. July 2013. ISBN 978-1-107-66182-0.
- Michael S. Diamond, Hannah M. Director, Ryan Eastman, Anna Possner, and Robert Wood. Substantial Cloud Brightening From Shipping in Subtropical Low Clouds. *AGU Advances*, 1(1):e2019AV000111, 2020. ISSN 2576-604X. doi: 10.1029/2019AV000111. URL <https://onlinelibrary.wiley.com/doi/abs/10.1029/2019AV000111>. eprint: <https://onlinelibrary.wiley.com/doi/pdf/10.1029/2019AV000111>.
- Tiantie Yuan, Hua Song, Robert Wood, Chenxi Wang, Lazaros Oreopoulos, Steven E. Platnick, Sophia von Hippel, Kerry Meyer, Siobhan Light, and Eric Wilcox. Global reduction in ship-tracks from sulfur regulations for shipping fuel. *Science Advances*, 8(29):eabn7988, July 2022. doi: 10.1126/sciadv.abn7988. URL <https://www.science.org/doi/full/10.1126/sciadv.abn7988>. Publisher: American Association for the Advancement of Science.
- P. A. Durkee, K. J. Noone, R. J. Ferek, D. W. Johnson, J. P. Taylor, T. J. Garrett, P. V. Hobbs, J. G. Hudson, C. S. Bretherton, G. Innis, G. M. Frick, W. A. Hoppel, C. D. O'Dowd, L. M. Russell, R. Gasparovic, K. E. Nielsen, S. A. Tessmer, E. Öström, S. R. Osborne, R. C. Flagan, J. H. Seinfeld, and H. Rand. The Impact of Ship-Produced Aerosols on the Microstructure and Albedo of Warm Marine Stratocumulus Clouds: A Test of MAST Hypotheses 1i and 1ii. *Journal of the Atmospheric Sciences*, 57(16):2554–2569, August 2000. ISSN 0022-4928, 1520-0469. doi: 10.1175/1520-0469(2000)057<2554:TIOSPA>2.0.CO;2. URL <https://journals.ametsoc.org/view/journals/atsc/57/16/1520-0469.2000.057.2554.tiospa.2.0.co.2.xml>. Publisher: American Meteorological Society Section: Journal of the Atmospheric Sciences.
- Lawrence F. Radke, James A. Coakley, and Michael D. King. Direct and Remote Sensing Observations of the Effects of Ships on Clouds. *Science*, 246(4934):1146–1149, December 1989. doi: 10.1126/science.246.4934.1146. URL <https://www.science.org/doi/10.1126/science.246.4934.1146>. Publisher: American Association for the Advancement of Science.
- Zhe Feng, L. Ruby Leung, Nana Liu, Jingyu Wang, Robert A. Houze Jr, Jianfeng Li, Joseph C. Hardin, Dandan Chen, and Jianping Guo. A Global High-Resolution Mesoscale Convective System Database Using Satellite-Derived Cloud Tops, Surface Precipitation, and Tracking. *Journal of Geophysical Research: Atmospheres*, 126(8):e2020JD034202, 2021. ISSN 2169-8996. doi: 10.1029/2020JD034202. URL <https://onlinelibrary.wiley.com/doi/abs/10.1029/2020JD034202>. eprint: <https://onlinelibrary.wiley.com/doi/pdf/10.1029/2020JD034202>.
- Wei-Kuo Tao, Jen-Ping Chen, Zhanqing Li, Chien Wang, and Chidong Zhang. Impact of aerosols on convective clouds and precipitation. *Reviews of Geophysics*, 50(2), 2012. ISSN 1944-9208. doi: 10.1029/2011RG000369. URL <https://onlinelibrary.wiley.com/doi/abs/10.1029/2011RG000369>. eprint: <https://onlinelibrary.wiley.com/doi/pdf/10.1029/2011RG000369>.
- Adele L. Igel and Susan C. van den Heever. Invigoration or Enervation of Convective Clouds by Aerosols? *Geophysical Research Letters*, 48(16):e2021GL093804, 2021. ISSN 1944-8007. doi: 10.1029/2021GL093804. URL <https://onlinelibrary.wiley.com/doi/abs/10.1029/2021GL093804>. eprint: <https://onlinelibrary.wiley.com/doi/pdf/10.1029/2021GL093804>.
- Adam C. Varble, Adele L. Igel, Hugh Morrison, Wojciech W. Grabowski, and Zachary J. Lebo. Opinion: A critical evaluation of the evidence for aerosol invigoration of deep convection. *Atmospheric Chemistry and Physics*, 23(21):13791–13808, November 2023. ISSN 1680-7316. doi: 10.5194/acp-23-13791-2023. URL <https://acp.copernicus.org/articles/23/13791/2023/>. Publisher: Copernicus GmbH.
- Joel A. Thornton, Katrina S. Virts, Robert H. Holzworth, and Todd P. Mitchell. Lightning enhancement over major oceanic shipping lanes. *Geophysical Research Letters*, 44(17):9102–9111, 2017. ISSN 1944-8007. doi: 10.1002/2017GL074982. URL <https://onlinelibrary.wiley.com/doi/abs/10.1002/2017GL074982>. eprint: <https://onlinelibrary.wiley.com/doi/pdf/10.1002/2017GL074982>.
- Tsutomoto Takahashi and Kuniko Miyawaki. Reexamination of Riming Electrification in a Wind Tunnel. *Journal of the Atmospheric Sciences*, 59(5):1018–1025, March 2002. ISSN 0022-4928, 1520-0469. doi: 10.1175/1520-0469(2002)059<1018:ROREIA>2.0.CO;2. URL <https://journals.ametsoc.org/view/journals/atsc/59/5/1520-0469.2002.059.1018.roreia.2.0.co.2.xml>. Publisher: American Meteorological Society Section: Journal of the Atmospheric Sciences.
- Wiebke Deierling, Walter A. Petersen, John Latham, Scott Ellis, and Hugh J. Christian. The relationship between lightning activity and ice fluxes in thunderstorms. *Journal of Geophysical Research: Atmospheres*, 113(D15), 2008. ISSN 2156-2202. doi: 10.1029/2007JD009700. URL <https://onlinelibrary.wiley.com/doi/abs/10.1029/2007JD009700>. eprint: <https://onlinelibrary.wiley.com/doi/pdf/10.1029/2007JD009700>.
- S. Twomey. The Influence of Pollution on the Shortwave Albedo of Clouds. *Journal of the Atmospheric Sciences*, 34(7):1149–1152, July 1977. ISSN 0022-4928, 1520-0469. doi: 10.1175/1520-0469(1977)034<1149:TIOPOP>2.0.CO;2. URL <https://journals.ametsoc.org/view/journals/atsc/34/7/1520-0469.1977.034.1149.tiopop.2.0.co.2.xml>. Publisher: American Meteorological Society Section: Journal of the Atmospheric Sciences.
- Edward R. Mansell and Conrad L. Ziegler. Aerosol Effects on Simulated Storm Electrification and Precipitation in a Two-Moment Bulk Microphysics Model. *Journal of the Atmospheric Sciences*, 70(7):2032–2050, July 2013. ISSN 0022-4928, 1520-0469. doi: 10.1175/JAS-D-12-0264.1. URL <https://journals.ametsoc.org/view/journals/atsc/70/7/jas-d-12-0264.1.xml>. Publisher: American Meteorological Society Section: Journal of the Atmospheric Sciences.
- Peter N. Blossy, Christopher S. Bretherton, Joel A. Thornton, and Katrina S. Virts. Locally Enhanced Aerosols Over a Shipping Lane Produce Convective Invigoration but Weak Overall Indirect Effects in Cloud-Resolving Simulations. *Geophysical Research Letters*, 45(17):9305–9313, 2018. ISSN 1944-8007. doi: 10.1029/2018GL078682. URL <https://onlinelibrary.wiley.com/doi/abs/10.1029/2018GL078682>. eprint: <https://onlinelibrary.wiley.com/doi/pdf/10.1029/2018GL078682>.
- Ruize Sun, Xiao Lu, Meng Gao, Yu Du, Haipeng Lin, Chris Wright, Cheng He, and Ke Yin. The impacts of shipping emissions on lightning: roles of aerosol-radiation-interactions and aerosol-cloud-interactions. *Environmental Research Letters*, 19(3):034038, February 2024. ISSN 1748-9326. doi: 10.1088/1748-9326/ad2aba. URL <https://dx.doi.org/10.1088/1748-9326/ad2aba>. Publisher: IOP Publishing.
- Tristan H. Abbott and Timothy W. Cronin. Aerosol invigoration of atmospheric convection through increases in humidity. *Science*, 371(6524):83–85, January 2021. doi: 10.1126/science.abc5181. URL <https://www.science.org/doi/full/10.1126/science.abc5181>. Publisher: American Association for the Advancement of Science.
- Jiwen Fan, Daniel Rosenfeld, Yuwei Zhang, Scott E. Giangrande, Zhanqing Li, Luiz A. T. Machado, Scot T. Martin, Yan Yang, Jian Wang, Paulo Artaxo, Henrique M. J. Barbosa, Ramon C. Braga, Jennifer M. Comstock, Zhe Feng, Wenhua Gao, Helber B. Gomes, Fan Mei, Christopher Pöhlker, Mira L. Pöhlker, Ulrich Pöschl, and Rodrigo A. F. de Souza. Substantial convection and precipitation enhancements by ultrafine aerosol particles. *Science*, 359(6374):411–418, January 2018. doi: 10.1126/science.aan8461. URL <https://www.science.org/doi/full/10.1126/science.aan8461>. Publisher: American Association for the Advancement of Science.
- Daniel Rosenfeld, Ulrike Lohmann, Graciela B. Raga, Colin D. O'Dowd, Markku Kulmala, Sandro Fuzzi, Anni Reissell, and Meinrat O. Andreae. Flood or Drought: How Do Aerosols Affect Precipitation? *Science*, 321(5894):1309–1313, September 2008. doi: 10.1126/science.1160606. URL <https://www.science.org/doi/full/10.1126/science.1160606>. Publisher: American Association for the Advancement of Science.
- IMO. IMO 2020 Cutting Sulphur Oxide Emissions, 2020. URL <https://www.imo.org/en/MediaCentre/HotTopics/Pages/Sulphur-2020.aspx>.
- Sami D. Seppälä, Joel Kuula, Antti-Pekka Hyvärinen, Sanna Saarikoski, Topi Rönkkö, Jorma Keskinen, Jukka-Pekka Jalkanen, and Hilikka Timonen. Effects of marine fuel sulfur restrictions on particle number concentrations and size distributions in ship plumes in the Baltic Sea. *Atmospheric Chemistry and Physics*, 21(4):3215–3234, March 2021. ISSN 1680-7316. doi: 10.5194/acp-21-3215-2021. URL <https://acp.copernicus.org/articles/21/3215/2021/>. Publisher: Copernicus GmbH.
- Duncan Watson-Parris, Matthew W. Christensen, Angus Laurenson, Daniel Clewley, Edward Gryspeird, and Philip Stier. Shipping regulations lead to large reduction in cloud perturbations. *Proceedings of the National Academy of Sciences*, 119(41):e2206885119, October 2022. doi: 10.1073/pnas.2206885119. URL <https://www.pnas.org/doi/abs/10.1073/pnas.2206885119>. Publisher: Proceedings of the National Academy of Sciences.
- Michael S. Diamond. Detection of large-scale cloud microphysical changes within a major shipping corridor after implementation of the International Maritime Organization 2020 fuel sulfur regulations. *Atmospheric Chemistry and Physics*, 23(14):8259–8269, July 2023. ISSN 1680-7316. doi: 10.5194/acp-23-8259-2023. URL <https://acp.copernicus.org/articles/23/8259/2023/>. Publisher: Copernicus GmbH.
- Port of Singapore. Bunkering Statistics, 2024. URL <https://www.mpa.gov.sg/port-marine-ops/marine-services/bunkering/bunkering-statistics>.
- Xiaoli Mao, Dan Rutherford, Liudmila Osipova, and Elise Georgeff. Exporting emissions: Marine fuel sales at the Port of Singapore. Technical report, July 2022.
- Cerdeiro, Komaromi, Liu, and Saeed. World Seaborne Trade in Real Time: A Proof of Concept for Building AIS-based Nowcasts from Scratch, 2020. URL <https://www.imf.org/en/Publications/WP/Issues/2020/05/14/World-Seaborne-Trade-in-Real-Time-A-Proof-of-Concept-for-Building-AIS-based-Nowcasts-from-49393>.
- George J. Huffman, David T. Bolvin, Dan Braithwaite, Kuolin Hsu, Robert Joyce, Pingping Xie, and Soo-Hyun Yoo. NASA global precipitation measurement (GPM) integrated multi-satellite retrievals for GPM (IMERG). *Algorithm theoretical basis document (ATBD) version*, 4(26):30, 2015. Publisher: NASA Goddard Space Flight Center Greenbelt, MD.
- Rajani Kumar Pradhan and Yannis Markonis. Performance Evaluation of GPM IMERG Precipitation Products over the Tropical Oceans Using Buoys. *Journal of Hydrometeorology*, 24(10):1755–1770, October 2023. ISSN 1525-7541, 1525-755X. doi: 10.1175/JHM-D-22-0216.1. URL <https://journals.ametsoc.org/view/journals/hydr/24/10/JHM-D-22-0216.1.xml>. Publisher: American Meteorological Society Section: Journal of Hydrometeorology.
- Daniel C. Watters, Patrick N. Gatlin, David T. Bolvin, George J. Huffman, Robert Joyce, Pierre Kirstetter, Eric J. Nelkin, Sarah Ringerud, Jackson Tan, Jianxin Wang, and David Wolff. Oceanic Validation of IMERG-GMI Version 6 Precipitation Using the GPM Validation Network.

- Journal of Hydrometeorology*, 25(1):125–142, December 2023. ISSN 1525-7541, 1525-755X. doi: 10.1175/JHM-D-23-0134.1. URL <https://journals.ametsoc.org/view/journals/hydr/25/1/JHM-D-23-0134.1.xml>. Publisher: American Meteorological Society Section: Journal of Hydrometeorology.
30. David M. Roms, Alexander B. Charn, Robert H. Holzworth, William E. Lawrence, John Molinari, and David Vollaro. CAPE Times P Explains Lightning Over Land But Not the Land-Ocean Contrast. *Geophysical Research Letters*, 45(22):12,623–12,630, 2018. ISSN 1944-8007. doi: 10.1029/2018GL080267. URL <https://onlinelibrary.wiley.com/doi/abs/10.1029/2018GL080267>. eprint: <https://onlinelibrary.wiley.com/doi/pdf/10.1029/2018GL080267>.
  31. Wei-Yi Cheng, Daehyun Kim, and Robert H. Holzworth. CAPE Threshold for Lightning Over the Tropical Ocean. *Journal of Geophysical Research: Atmospheres*, 126(20):e2021JD035621, 2021. ISSN 2169-8996. doi: 10.1029/2021JD035621. URL <https://onlinelibrary.wiley.com/doi/abs/10.1029/2021JD035621>. eprint: <https://onlinelibrary.wiley.com/doi/pdf/10.1029/2021JD035621>.
  32. Yannian Zhu, Daniel Rosenfeld, and Zhanqing Li. Under What Conditions Can We Trust Retrieved Cloud Drop Concentrations in Broken Marine Stratocumulus? *Journal of Geophysical Research: Atmospheres*, 123(16):8754–8767, 2018. ISSN 2169-8996. doi: 10.1029/2017JD028083. URL <https://onlinelibrary.wiley.com/doi/abs/10.1029/2017JD028083>. eprint: <https://onlinelibrary.wiley.com/doi/pdf/10.1029/2017JD028083>.
  33. Michael Peterson. Interactions Between Lightning and Ship Traffic. *Earth and Space Science*, 10(11):e2023EA002926, 2023. ISSN 2333-5084. doi: 10.1029/2023EA002926. URL <https://onlinelibrary.wiley.com/doi/abs/10.1029/2023EA002926>. eprint: <https://onlinelibrary.wiley.com/doi/pdf/10.1029/2023EA002926>.
  34. Richard L Dowden, James B Brundell, and Craig J Rodger. VLF lightning location by time of group arrival (TOGA) at multiple sites. *Journal of Atmospheric and Solar-Terrestrial Physics*, 64(7):817–830, May 2002. ISSN 1364-6826. doi: 10.1016/S1364-6826(02)00085-8. URL <https://www.sciencedirect.com/science/article/pii/S1364682602000858>.
  35. Hans Hersbach, Bill Bell, Paul Berrisford, Shoji Hirahara, András Horányi, Joaquín Muñoz-Sabater, Julien Nicolas, Carole Peubey, Raluca Radu, Dinand Schepers, Adrian Simmons, Cornel Soci, Saleh Abdalla, Xavier Abellan, Gianpaolo Balsamo, Peter Bechtold, Gionata Biavati, Jean Bidlot, Massimo Bonavita, Giovanna De Chiara, Per Dahlgren, Dick Dee, Michail Diamantakis, Rossana Dragani, Johannes Flemming, Richard Forbes, Manuel Fuentes, Alan Geer, Leo Haimberger, Sean Healy, Robin J. Hogan, Elías Hólm, Marta Janisková, Sarah Keeley, Patrick Laloyaux, Philippe Lopez, Cristina Lupu, Gabor Radnoti, Patricia de Rosnay, Iryna Rozum, Freja Vamborg, Sebastien Villaume, and Jean-Noël Thépaut. The ERA5 global reanalysis. *Quarterly Journal of the Royal Meteorological Society*, 146(730):1999–2049, 2020. ISSN 1477-870X. doi: 10.1002/qj.3803. URL <https://onlinelibrary.wiley.com/doi/abs/10.1002/qj.3803>. eprint: <https://onlinelibrary.wiley.com/doi/pdf/10.1002/qj.3803>.
  36. National Center for Atmospheric Research Staff (Eds). The Climate Data Guide: Regridding Overview, 2014. URL <https://climatedataguide.ucar.edu/climate-tools/regridding-overview>.
  37. Monica Crippa, Greet Janssens-Maenhout, Frank Dentener, Diego Guizzardi, Katerina Sindelarova, Marilena Muntean, Rita Van Dingenen, and Claire Granier. Forty years of improvements in European air quality: regional policy-industry interactions with global impacts. *Atmospheric Chemistry and Physics*, 16(6):3825–3841, March 2016. ISSN 1680-7316. doi: 10.5194/acp-16-3825-2016. URL <https://acp.copernicus.org/articles/16/3825/2016/>. Publisher: Copernicus GmbH.
  38. Yang Cao, Yannian Zhu, Minghui Wang, Daniel Rosenfeld, Yuan Liang, Jihu Liu, Zhoukun Liu, and Hemin Bai. Emission Reductions Significantly Reduce the Hemispheric Contrast in Cloud Droplet Number Concentration in Recent Two Decades. *Journal of Geophysical Research: Atmospheres*, 128(2):e2022JD037417, 2023. ISSN 2169-8996. doi: 10.1029/2022JD037417. URL <https://onlinelibrary.wiley.com/doi/abs/10.1029/2022JD037417>. eprint: <https://onlinelibrary.wiley.com/doi/pdf/10.1029/2022JD037417>.
  39. Avichay Efraim, Daniel Rosenfeld, Julia Schmale, and Yannian Zhu. Satellite Retrieval of Cloud Condensation Nuclei Concentrations in Marine Stratocumulus by Using Clouds as CCN Chambers. *Journal of Geophysical Research: Atmospheres*, 125(16):e2020JD032409, 2020. ISSN 2169-8996. doi: 10.1029/2020JD032409. URL <https://onlinelibrary.wiley.com/doi/abs/10.1029/2020JD032409>. eprint: <https://onlinelibrary.wiley.com/doi/pdf/10.1029/2020JD032409>.
  40. Yichuan Wang, Yannian Zhu, Minghui Wang, Daniel Rosenfeld, Yang Gao, Xiaohong Yao, Lifang Sheng, Avichay Efraim, and Juntao Wang. Validation of satellite-retrieved CCN based on a cruise campaign over the polluted Northwestern Pacific ocean. *Atmospheric Research*, 260:105722, October 2021. ISSN 0169-8095. doi: 10.1016/j.atmosres.2021.105722. URL <https://www.sciencedirect.com/science/article/pii/S0169809521002787>.
  41. Ralf Bennartz and John Rausch. Global and regional estimates of warm cloud droplet number concentration based on 13 years of AQUA-MODIS observations. *Atmospheric Chemistry and Physics*, 17(16):9815–9836, August 2017. ISSN 1680-7316. doi: 10.5194/acp-17-9815-2017. URL <https://acp.copernicus.org/articles/17/9815/2017/acp-17-9815-2017.html>. Publisher: Copernicus GmbH.
  42. Daniel P. Grosvenor, Odran Sourdeval, Paquita Zuidema, Andrew Ackerman, Mikhail D. Alexandrov, Ralf Bennartz, Reinout Boers, Brian Cairns, J. Christine Chiu, Matthew Christensen, Hartwig Deneke, Michael Diamond, Graham Feingold, Ann Fridlind, Anja Hünerbein, Christine Knist, Pavlos Kollias, Alexander Marshak, Daniel McCoy, Daniel Merk, David Painemal, John Rausch, Daniel Rosenfeld, Herman Russchenberg, Patric Seifert, Kenneth Sinclair, Philip Stier, Bastiaan van Dierenhoven, Manfred Wendisch, Frank Werner, Robert Wood, Zhibo Zhang, and Johannes Quaas. Remote Sensing of Droplet Number Concentration in Warm Clouds: A Review of the Current State of Knowledge and Perspectives. *Reviews of Geophysics*, 56(2):409–453, 2018. ISSN 1944-9208. doi: 10.1029/2017RG000593. URL <https://onlinelibrary.wiley.com/doi/abs/10.1029/2017RG000593>. eprint: <https://onlinelibrary.wiley.com/doi/pdf/10.1029/2017RG000593>.
  43. Chris Wright. Lightning Declines Over Shipping Lanes Follow Regulation of Fuel Sulfur: Data Analysis, May 2024. URL <https://zenodo.org/records/11373991>.



**Supplemental Information for: Lightning declines over shipping lanes following regulation of fuel sulfur emissions**

DRAFT

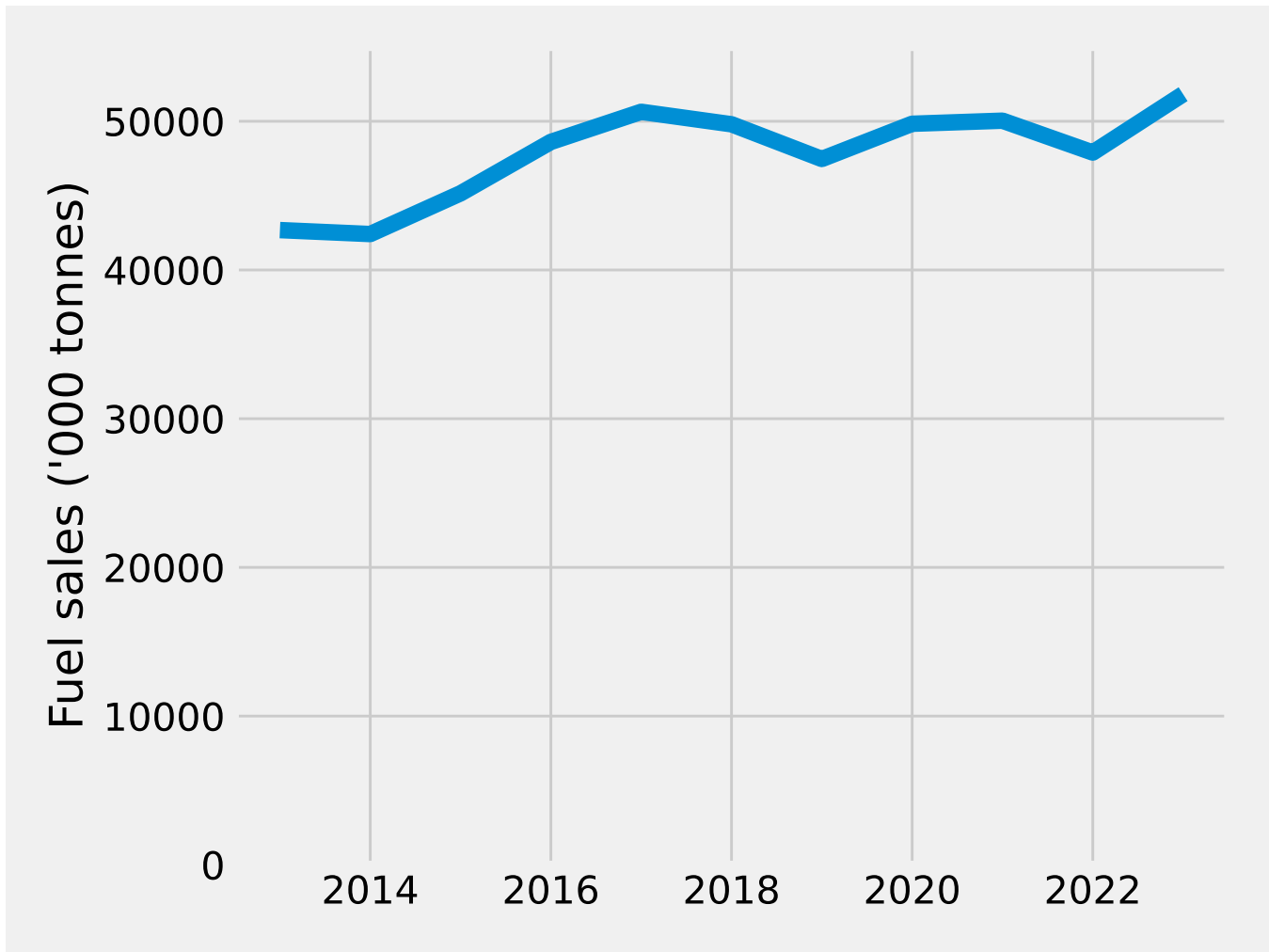


**Fig. S1.** Total fuel sales at the Port of Singapore have been generally increasing in this region

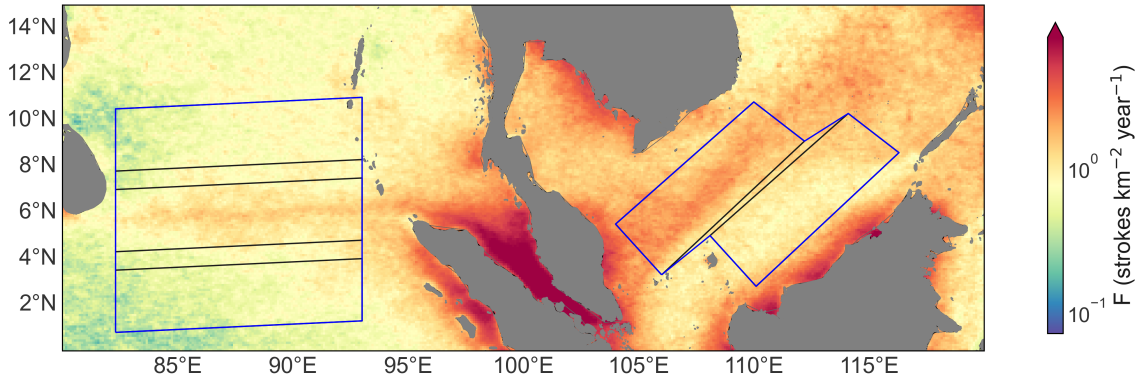


**Fig. S2.** Climatology as in Figure 1, but with the boxes used for CAPE-Precipitation enhancement calculations (black). Our approach differs slightly from that of Thornton et al., (2017), in that only the Southern Indian Ocean reference region is used for CAPE-Precip analysis due to its similarity to the Indian Ocean shipping lane in frequency of convection and precipitation during the high-lightning season (November to April). Conducting the same analysis with the Northern Indian Ocean reference region does not alter the conclusions of this analysis. Blue boxes show regions used for compositing lightning and  $N_d$  as a function of distance from the shipping lane

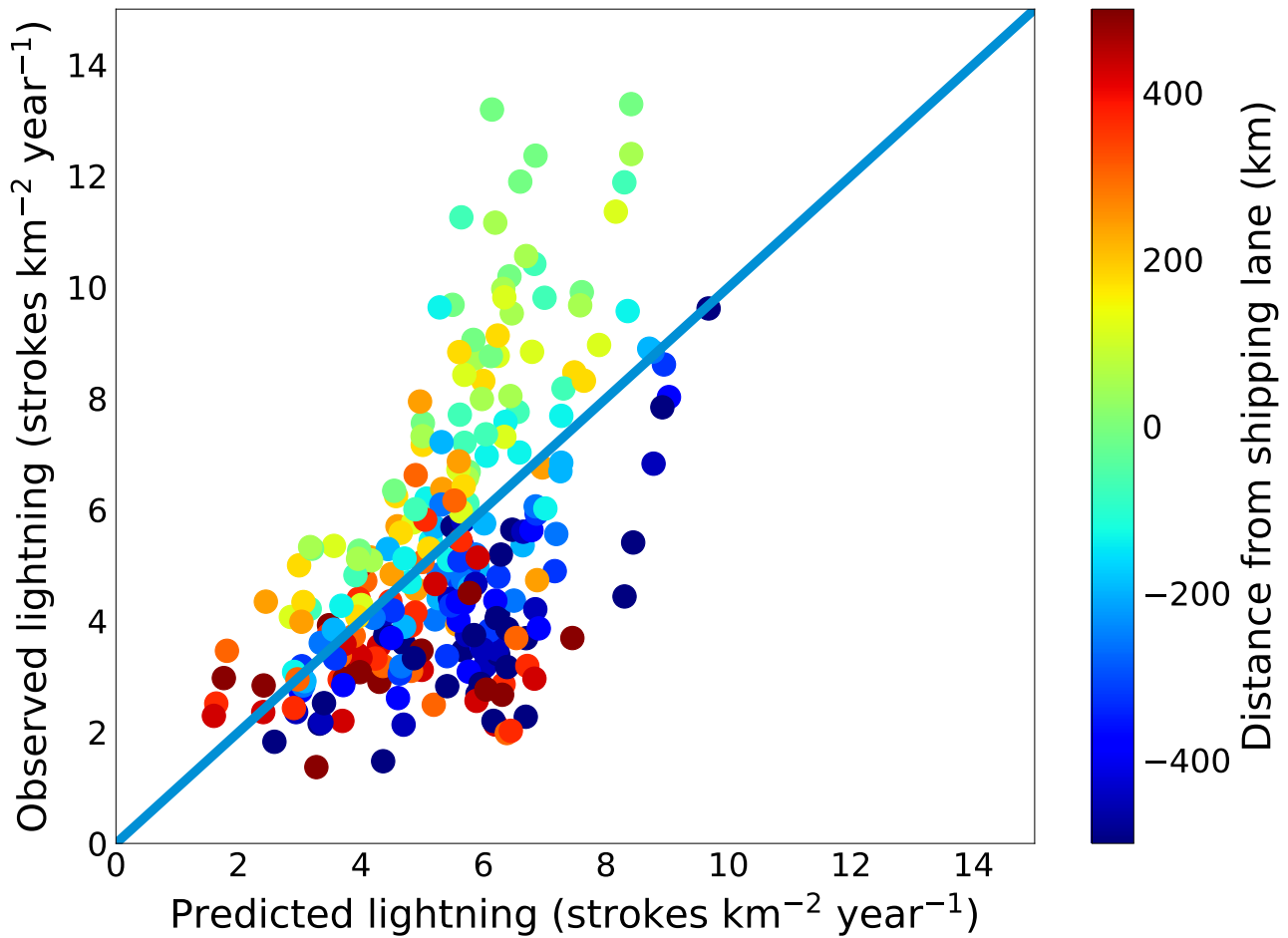


**Fig. S3.** Observed vs predicted lightning stroke density. Predictions are from linear regression of lightning stroke density against CAPE, precipitation, and ONI. Colors show the distance from the shipping lane.  $R^2$  is 0.33.

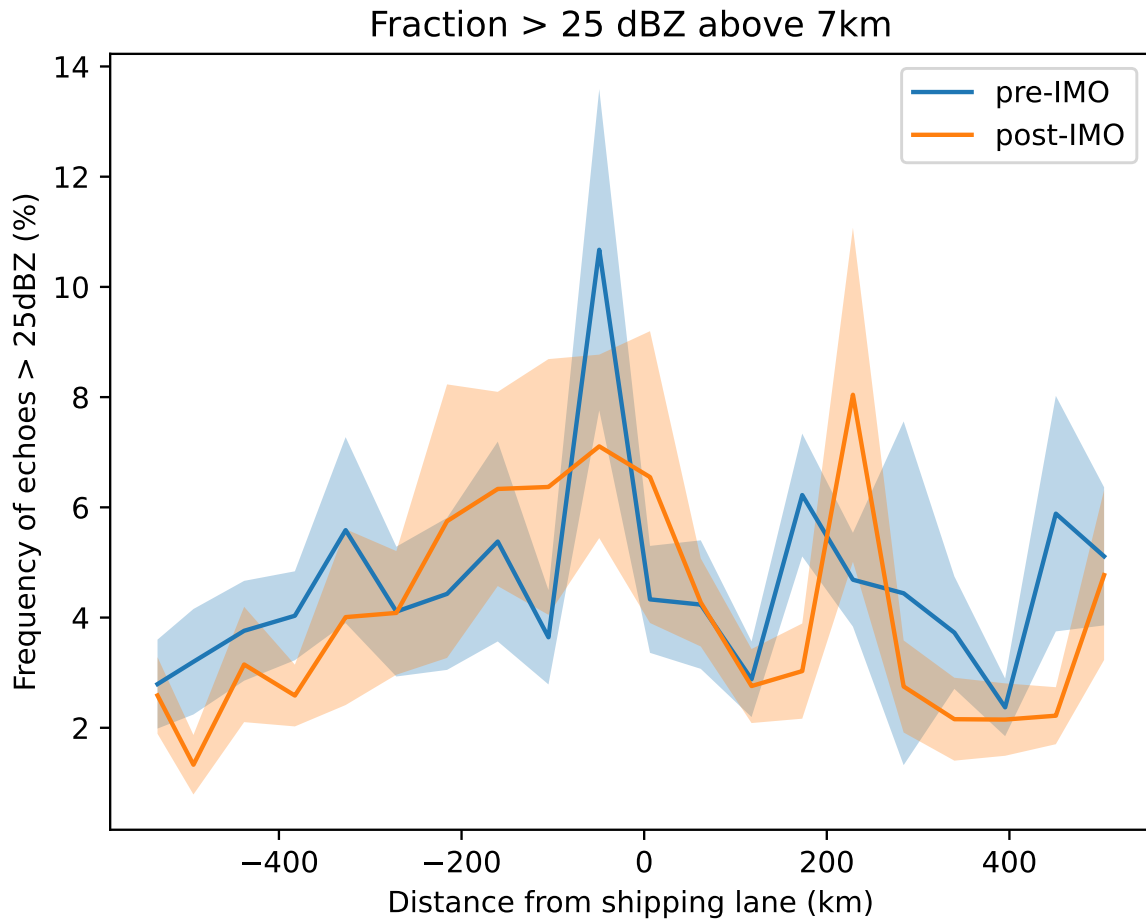


**Fig. S4.** Frequency of cold echoes (25dBZ or greater, above 8km), discussed in Blossey et al (2018) and citations therein as a proxy for lightning. The peak in reflectivity has diminished since the regulation, but weak sampling power does not allow us to confirm this change.

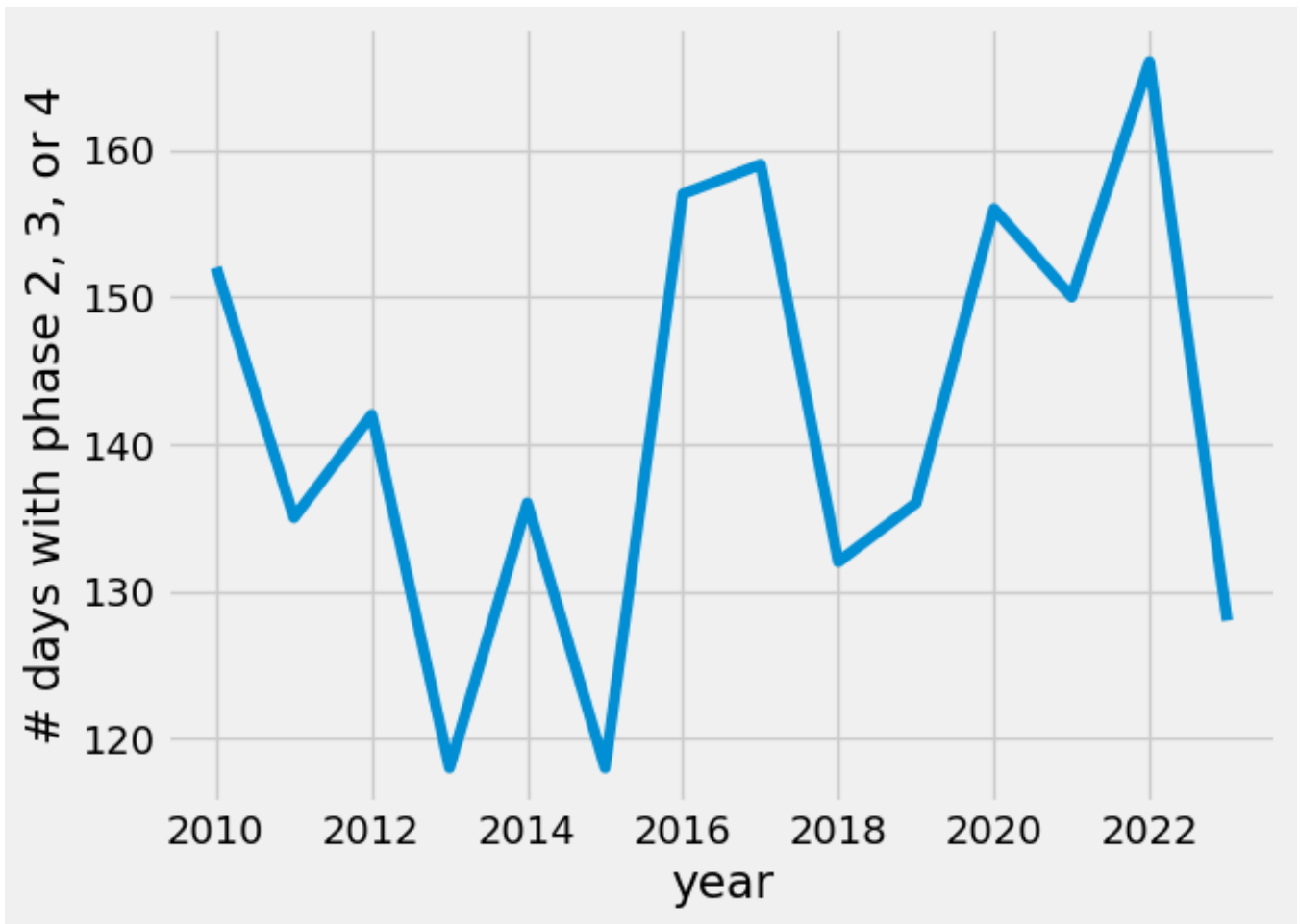


**Fig. S5.** Number of days with MJO phase 2, 3, or 4 from Realtime Multivariate MJO Index (RMM). This indicator of intraseasonal variability shows no clear trend since 2020



DRAFT